論 文

A Study on Solidification and Wear Character of Multi-alloyed White Cast Iron

Sung-Kon Yu and Yasuhiro Matsubara*

초 록

응고 및 마모거동을 연구하기 위하여 Cr, V, Mo 및 W의 조성이 다른 3종류의 백주철을 주조하였다. 고주파유도용해로에서 장입시켜 1873K까지 승온시켜 장입원료들을 모두 용해시킨 후 1823K에서 Y블럭주형에 주입하였다. 얻어진 3종류의 백주철조성은 다음과 같다: Fe-3%C-10%Cr-5%Mo-5%W(합금1), Fe-3%C-10%V-5%Mo-5%W(합금2) 및 Fe-3%C-17%Cr-3%V(합금 3)응고과정을 추적하기 위하여 각 시편으로부터 50 g을 채취한 후 알루미나도가니에 넣고 실리콘카바이드로를 사용하여 1723K의 알콘분위기하에서 재용해를 시켰다. 용금을 10K/분의 속도로 냉각시키면서 열분석을 행하였으며 도중 몇 차례 소입실험을 병행하였다.합금1의 경우 초정오스테나이트, (오스테나이트+M_7C_3)공정, (오스테나이트+M_6C)공정, 합금2의 경우 초정 MC, 초정오스테나이트, (오스테나이트+MC)공정, (오스테나이트+M_2C)공정, 합금3의 경우 초정 $M7C_3$와 (오스테나이트+M_7C_3)공정으로 구성되어 있었다. 주방상태, 균질화열처리상태, 공냉상태, 템퍼링상태에서 내마모시험을 행하였다. 먼저 주방상태시편을 진공분위기하에서 1223K에서 5시간동안 균질화열처리를 행한후 로냉을 시켰다. 다시 이 시편을 1323K에서 2시간 유지 후 강제공냉을 시켰으며 강제공냉된 시편을 573K에서 3시간동안 템퍼링처리를 하였다. 내마모시험은 120 mesh마모지에 10N의 하중을 가하여 실시하였다. 각 사이클마다 무게감소를 측정하였으며 8번 반복실험을 하였다. 마모량은 균질화열처리시편, 주방상태시편, 템퍼링시편, 공냉시편의 순으로 감소하였다. 합금2가 마모량이 가장 적었으며 합금3이 가장 많았다. 합금2의 마모량이 가장 적은 이유는 조직이 초정 MC, 공정 MC 및 공정 M2C로 구성되어 있기 때문으로 사료된다.주방상태에서 기지조직은 퍼얼라이트이었으나 열처리를 통하여 마르텐사이트, 템퍼드마르텐사이트, 잔류오스테나이트로 변태하였다. 이상의 결과를 종합해 보면 MC가 내마모성에 가장 기여하는 조직으로 판단되어진다.

(Received Jul 12, 2000)

1. Introduction

Alloyed white cast iron with many kinds of strong carbide-forming elements is a recently developed wear resistant material for the application to the hot strip and mineral pulverizing mills[1-11]. It contains reasonable amounts of elements, such as Cr, V, Mo, W and Nb, and the carbon content is relatively higher than that of high-speed tool steel with similar alloying elements. MC, M_2C, M_6C, M_7C_3 and NbC carbides can be precipitated as primary and/or eutectic carbides during solidification. In addition, the matrix can also be varied by the heat-treatments such as air-hardening and tempering, and particularly hard matrix can be obtained due to the precipitation of numerous minute secondary carbides and the transformation of martensite from retained austenite.

Properties such as abrasion wear resistance, surface roughening resistance and seizing or sticking resistance are essentially important to apply these alloyed white cast irons for the rolls and other wear resistant parts of steel rolling and mineral pulverizing mills. Among these properties, the abrasion wear resistance is reported to be dependent upon not only type, morphology, amount and distribution pattern of the carbides precipitated from the melt, but also the type of matrix structure. Neverthless, the abrasion wear resistance of these irons was little researched systematically.

In this work, alloyed white cast irons with three di-

Dept. of Materials Engineering, Keimyung University, 1000 shindang-Dong, Dalseo-Ku, Taegu, 704-701, Korea
*Dept. of Materials Science and Metallurgical Engineering, Kurume National College of Technology, 1 -1-1 Komorino, Kurume 830-8555, Japan

fferent chemical compositions were selected for the investigation of solidification and abrasion wear resistance. In order to clarify the solidification process, the specimen was quenched into water from different temperatures during thermal analysis to interrupt freezing. On the other hand, heat-treatments such as air-hardening and tempering were employed to obtain the different type of matrix structures. Then, the effect of carbide type and matrix structure on the abrasion wear resistance was investigated using a scratching type abrasion wear testing machine. The worn parts of the specimens were also examined by the scanning electron microscope(SEM) to derive the mechanism of abrasion wear.

2. Experimental Procedure

2.1 Specimen Preparation

To obtain the alloys with several combinations of the different carbides, the four alloying elements such as Cr, Mo, W and V were designed so as to make their sum approximately 20 mass%. The alloys were melted in a 15kg-capacity high frequency induction furnace. Initial charge materials were clean pig iron and steel scrap. Ferro-alloys such as Fe-60%Cr, Fe-80%V, Fe-60%Mo and Fe-75%W were added to a slag-free molten iron so as to minimize the oxidation loss and the slag formation. The melt was subsequently super-heated to 1873K and transferred into a pre-heated teapot ladle. After removal of any dross and slag, the melt was poured at 1823K into the pepset molds to produce Y-block ingots. The chemical analysis and co-existent carbides of the alloys are shown in Table 1.

2.2 Thermal Analysis

For studying the solidification sequence of each alloy, 50g were remelted at 1723K in an alumina crucible using a silicon carbide resistance furnace under argon atmosphere. Then, the molten iron was cooled at the rate of 10 K/min to reveal all the solidification reactions of the alloy through a cooling curve. Based upon the cooling curve, the molten iron was quenched into water from several temperatures on the way of thermal analysis.

Table 1. Chemical composition and co-existent carbides of the alloys.

Alloy No.	Element (mass%)					Cabide Type
	C	Cr	V	Mo	W	
1	2.98	9.95	0.01	5.14	4.87	M_7C_3, M_6C
2	3.04	0.04	10.21	5.21	4.84	MC, M_2C
3	3.07	17.54	3.14	0.01	0.02	M_7C_3

2.3 Heat-Treatment

Before air-hardening and tempering, the as-cast specimens were homogenized at 1223K for 5h under vacuum atmosphere. Then, they were air-hardened in forced air after austenitizing at 1323K for 2h in vacuum atmosphere and followed by tempering at 573K for 3h.

2.4 Measurement of Austenite

The volume fraction of austenite was calculated from the ratio of peak areas of (200) and (220) for ferrite(α) and martensite(M), and those of (220) and (311) for austenite(γ). The diffraction patterns were obtained by employing a simultaneous rotating and swinging sample stage in order to minimize or cancel the effect of texture. The X-ray diffraction was carried out by using Mo-Kα line with Zr filter and diffracting the angle(2θ) from 24 to 44 degree.

2.5 Wear Test

A schematic drawing of a main portion of the abrasion wear testing machine is illustrated in Fig. 1. Under the 10N load, the abrading wheel(44 mm in diameter and 12 mm in thickness) wound the circumference with 120 mesh SiC abrasive paper was revolved intermittently while moving back and forth by 35 mm stroke on

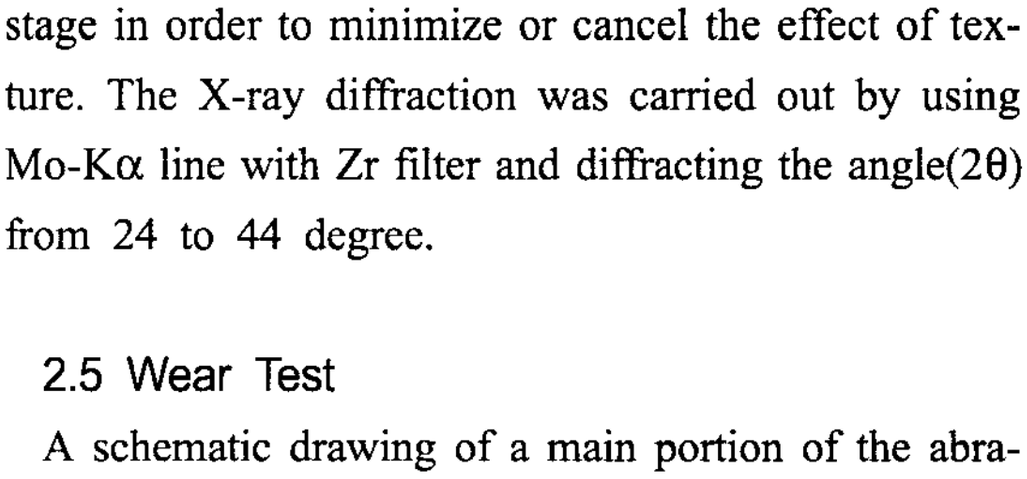

Fig. 1. A schematic drawing of abrasion wear testing machine.

the same area of the test piece in dry condition. The revolving speed of the abrading wheel was 0.345 mm/s and the worn area on the specimen was 420(12× 35 mm)mm^2. The wear loss of the test piece was measured after each cycle, which was taken 400s/cycle and this procedure was repeated up to 8 cycles.

2.6 Metallographic Examination

The specimens were polished, etched and examined metallographically by OM and SEM.

Villela's and Murakami's etchants were employed to distinguish the phases clearly.

3. Results and Discussion

3.1 Solidification Process

Since the multi-component white cast irons contain plural elements with strong carbide forming ability and there exists no phase diagram of such multi-component system, it is difficult to estimate their solidification process from the as-cast structure. The technique that a sample is quenched into water from temperatures before and after the reaction point during thermal analysis has been successfully employed to reveal the solidification sequence of cast alloys because the freezing process is *interrupted by quenching*[12].

A cooling curve of the alloy No.1 with six different quenching temperatures and the corresponding microstructures are shown in Fig. 2. On the cooling curve, three reaction or arrest points indicated by R_1, R_2, R_3 appeared at 1418, 1413 and 1363K. The determination of solidification reaction at each arrest was carried out by observing the microstructure of the quenched specimens. A microstructure quenched at 1593K as shown in Fig.2①, consists of very fine structure with dendritic austenite, and this proves that the structure was formed directly from a liquid state. At the first arrest(R_1) on the cooling curve, significant undercooling and recalescence were detected. Therefore, two quenching tests were conducted around there, at 1428K just prior to the start of the first arrest and at 1420K just after it. As shown in Fig. 2② and ③, both microstructures are similar in morphology having a little grown primary austenite dendrites and very fine structure filled in the interdendrites. The microstructure of Fig. 2④ quenched from 1410K that was just after the second arrest(R_2), consists of developed primary γ, (γ + M_7C_3) eutectic and re-mained liquid which is seen as the minute structure. The (γ + M_7C_3) eutectic are on the way of growing. This (γ + M_7C_3) eutectic in colony morphology was already reported in the solidification of high chromium white iron[12]. From these results, the first arrest is considered to be a precipitation of primary γ and the second arrest to be (γ + M_7C_3) eutectic reaction. The micro-

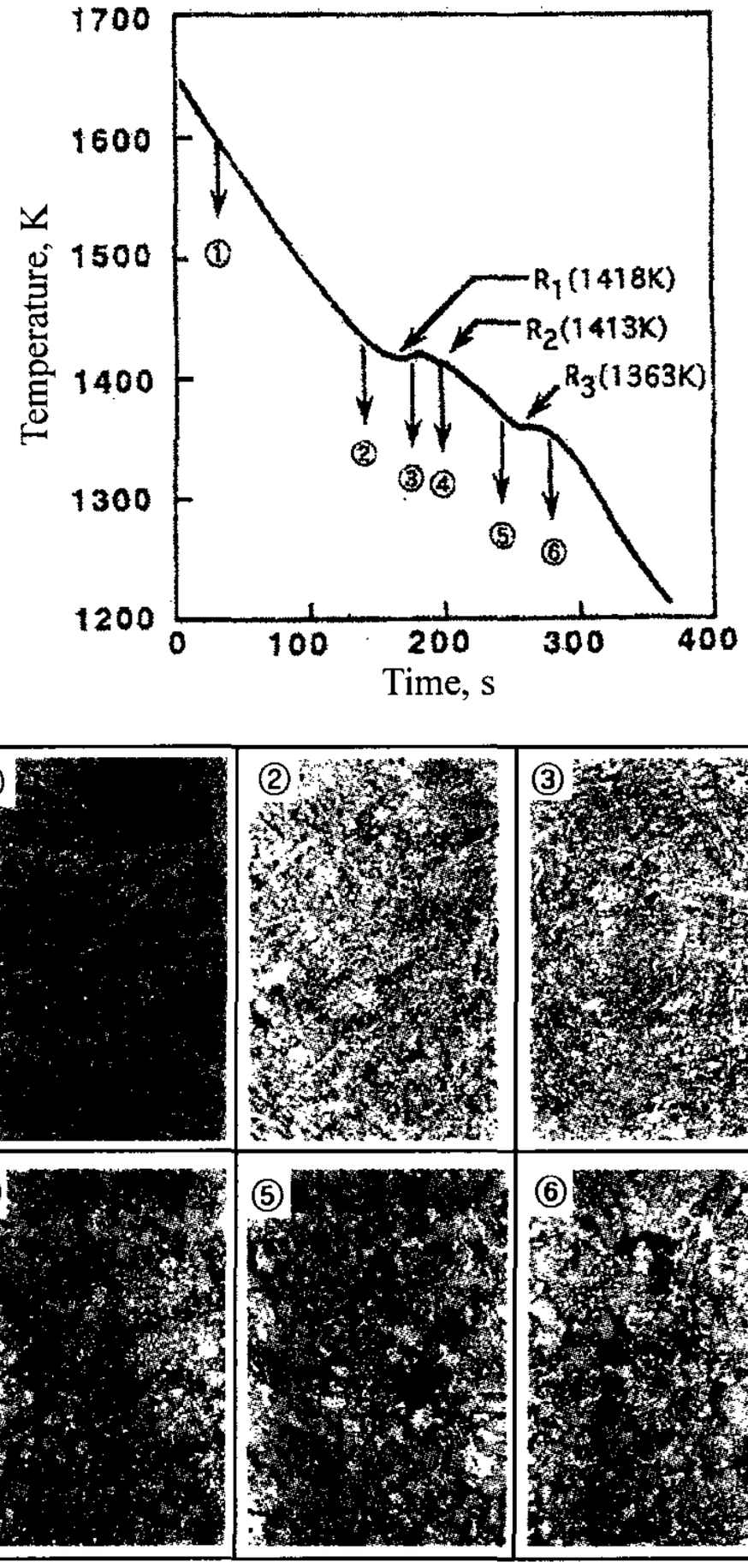

Fig. 2. A thermal analysis curve(top) and microstructures (bottom) quenched from different temperatures during solidification of alloy No.1.

structure of a specimen quenched at 1368K before the third arrest(R_3) is shown in Fig. 2⑤. It consists of primary γ, ($\gamma + M_7C_3$) eutectic, a little developed eutectic structure in a fish-bone shape and the former liquid part. When the microstructure of the specimen ⑤ is compared with that of the specimen ⑥ quenched after the third arrest or the final reaction, it is clear that the liquid phase is nearly disappeared in Fig. 2⑥ and in stead the eutectic structure in fish-bone morphology is apparently distinguished. This fish-bone carbide is well-known as a typical M_6C carbide formed by the addition of Mo and W elements[13,14]. So, the third arrest is considered to be the reaction of ($\gamma + M_6C$) eutectic. Therefore, the solidification process of this alloy starts with precipitation of primary γ, followed by that of ($\gamma + M_7C_3$) eutectic and finally ($\gamma + M_6C$) eutectic.

A cooling curve of the alloy No.2 with six quenching temperatures and the corresponding microstructures are shown in Fig. 3. On the cooling curve, three reaction points indicated by R_1, R_2, R_3 appeared at 1548, 1538 and 1408K. The microstructure quenched from 1623K, as shown in Fig. 3①, consists of the grown primary MC carbides in nodular shape and very fine structure that was rapidly frozen from liquid. Therefore, the reaction or arrest due to the precipitation of the primary MC carbide took place at much higher temperature than that of the initially quenched temperature of 1623K. Microstructure ② quenched from 1553K just before the first arrest(R_1) shows primary MC carbide, a little developed austenite dendrite and very fine structure which was in the liquid state. This suggest that the first arrest is the reaction of precipitation of primary austenite. The microphotograph ③ quenched at 1533K just after the second arrest(R_2) consists of primary MC carbide, austenite dendrite, ($\gamma + MC$) eutectic and the former liquid part, as shown in Fig. 3③. When the microstructure ③ is compared with the microstructure ④ obtained by quenching from 1518K, it can be seen that ($\gamma + MC$) eutectic is growing in cellular shape from the circumference of primary MC carbides. However, the liquid phase still remains in the specimen ④. The specimen ⑤ quenched from 1428K that is just before the third arrest(R_3) has a

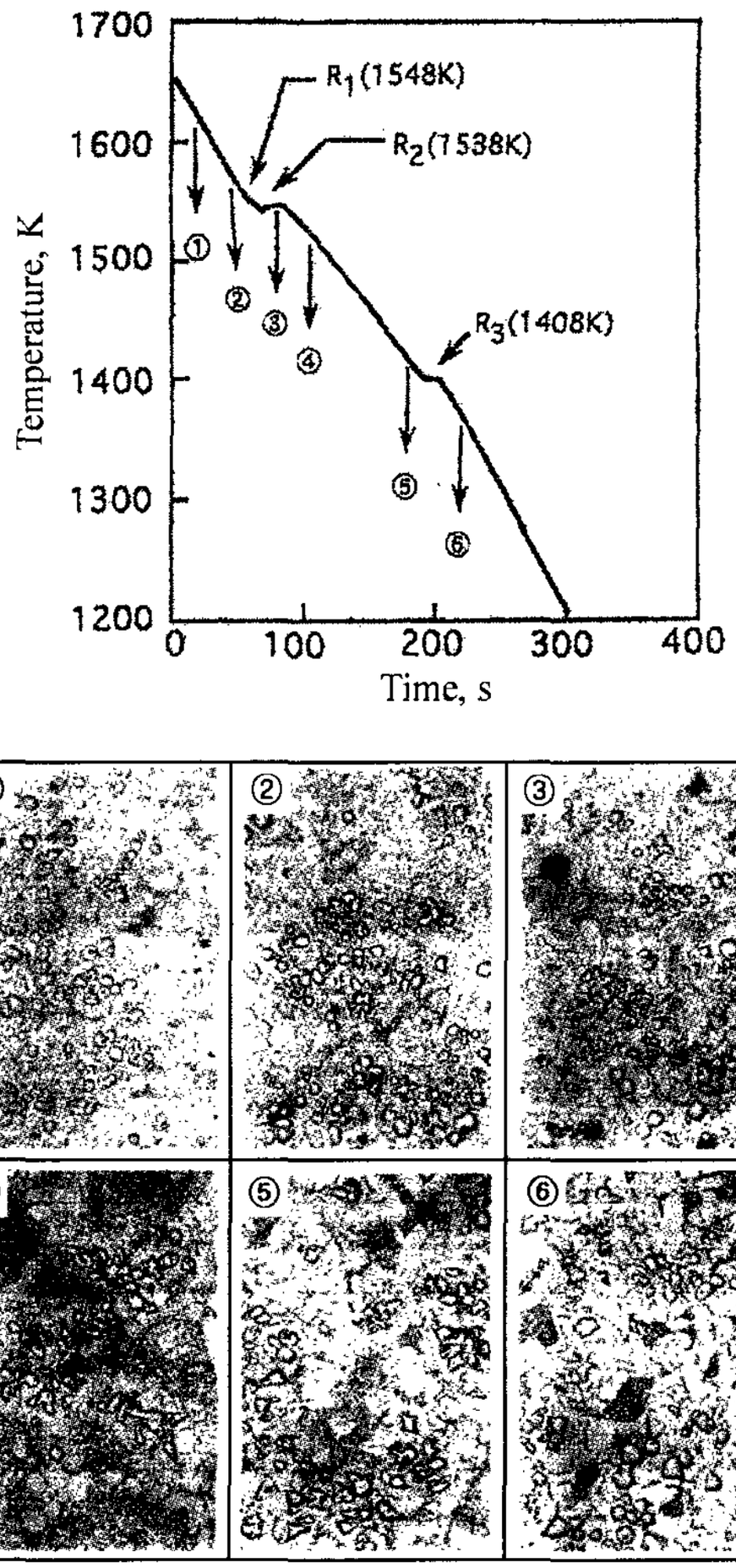

Fig. 3. A thermal analysis curve(top) and microstructures (bottom) quenched from different temperatures during solidification of alloy No.2.

microstructure with primary MC carbides and austenite dendrite, grown ($\gamma + MC$) eutectic and reduced amounts of remained liquid. From the microstructure⑥ quenched at 1378K after the third arrest, it is clear that the liquid part existed in the specimen ⑤ is gone and instead a lamellar eutectic structure of ($\gamma + M_2C$) appears, which is frequently observed in high speed tool steels and multi-component white cast irons[14]. Usually, the M_2C and M_6C carbides are formed by the addition of Mo and W elements, and then, the third arrest is considered to be a reaction of ($\gamma + M_2C$) eutectic solidification. From above results, the solidification sequence of the alloy

No.2 starts with the precipitation of primary MC carbide from the melt at very high temperature followed by precipitation of austenite dendrite. Then, (γ+MC) eutectic forms in the remained liquid and finally (γ+M_2C) eutectic solidifies.

Alloy No.3 is so called a high chromium white cast iron. From the many publications on the solidification of high chromium cast iron, the solidification sequence of the alloy No.3 can be explained that the primary M_7C_3 carbide in hexagonal morphology solidifies first and (γ+M_7C_3) eutectic solidification follows in the remained liquid. In this alloy, (γ+MC) eutectic solidification did not occur because of lower V content.

3.2 Abrasion Wear Behavior in As-cast State

For later discussions, the volume fraction of austenite in matrix(Vr), that of carbide in alloy(Vc) and the macrohardness(HV30) for as-cast(AS), homogenized(AH), air-hardened(AHF), and hardened-tempered(AHFT) specimens are summarized in Table 2. The abrasion wear test result of each alloy in the as-cast state is shown in Fig. 4. Since nearly linear relations are obtained between wear loss and testing time in all the specimens, it is convenient to adopt the term "wear rate(Rw: mg/s)" which is expressed by the slope of each straight line. As shown in Fig. 4, the range of Rw values in the as-cast specimens was from 0.030 to 0.045 mg/s depending upon the alloy type. The lowest Rw value, which means the highest abrasion wear resistance, was obtained in the alloy No.2 which contains high V and consists of primary MC carbide, eutectic MC carbide, lamellar M_2C carbide and pearlitic matrix. The alloy No.3, which showed the worst abrasion wear resistance, has a microstructure

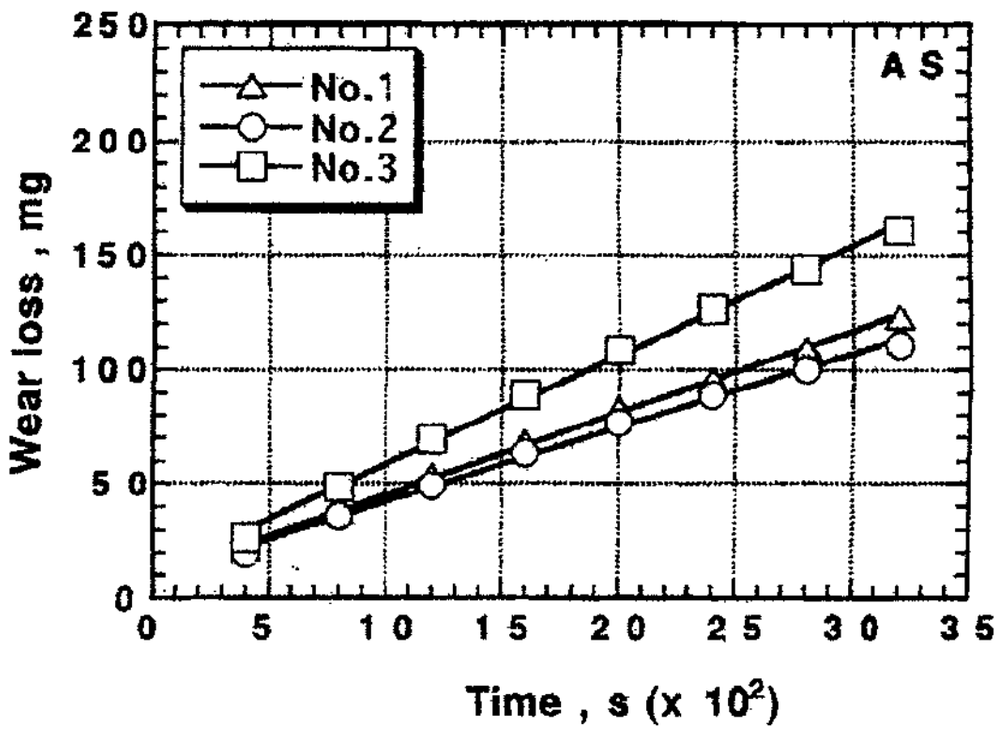

Fig. 4. Relationship between wear loss and testing time in as-cast(AS) state.

with primary M_7C_3 carbide, eutectic M_7C_3 carbide and pearlitic matrix. On the other hand, the Rw value of the alloy No.1 ranked between the alloys No.2 and No.3, consisting of eutectic M_7C_3 carbide, eutectic M_6C carbide and pearlitic matrix. Because the as-cast matrix structures in the three alloys are all pearlitic in common as shown in Fig. 5(a), it can be said that the abrasion wear resistance in the as-cast state depends mainly upon the type, morphology and amount of carbides. As shown in Table 2, the volume fraction of carbide of the alloy No.1 is the highest and that of the alloy No.2 is the lowest, and the macrohardness of the alloy No.2 is also the lowest among the three alloys. In spite of the lowest volume fraction of carbides and macrohardness, the highest wear resistance was obtained in the alloy No.2. This could be attributed to the fact that the main carbide types of this alloy are MC which has the highest hardness among the carbides in alloyed white cast iron, and M_2C with considerable amounts of W which is hardest next to the MC carbide. On the other hand, the alloy

Table 2. Effects of heat-treatment condition on volume fraction of austenite (V_γ) and carbide (V_C), and macrohardness (HV30).

Specimen / Item / Heat-treatment	Alloy No.1			Alloy No.2			Alloy No.3		
	V_γ(%)	V_C(%)	HV30	V_γ(%)	V_C(%)	HV30	V_γ(%)	V_C(%)	HV30
AS (As-cast)	0.2	32.9	652	0.2	15.8	514	0.4	29.9	842
AH (Homogenizing)	0.2	32.9	554	0.2	15.8	449	0.3	29.9	593
AHF (Air-hardening)	25.3	32.9	905	10.9	15.8	695	6.9	29.9	912
AHFT (Tempering)	21.5	32.9	905	7.2	15.8	666	5.4	29.9	842

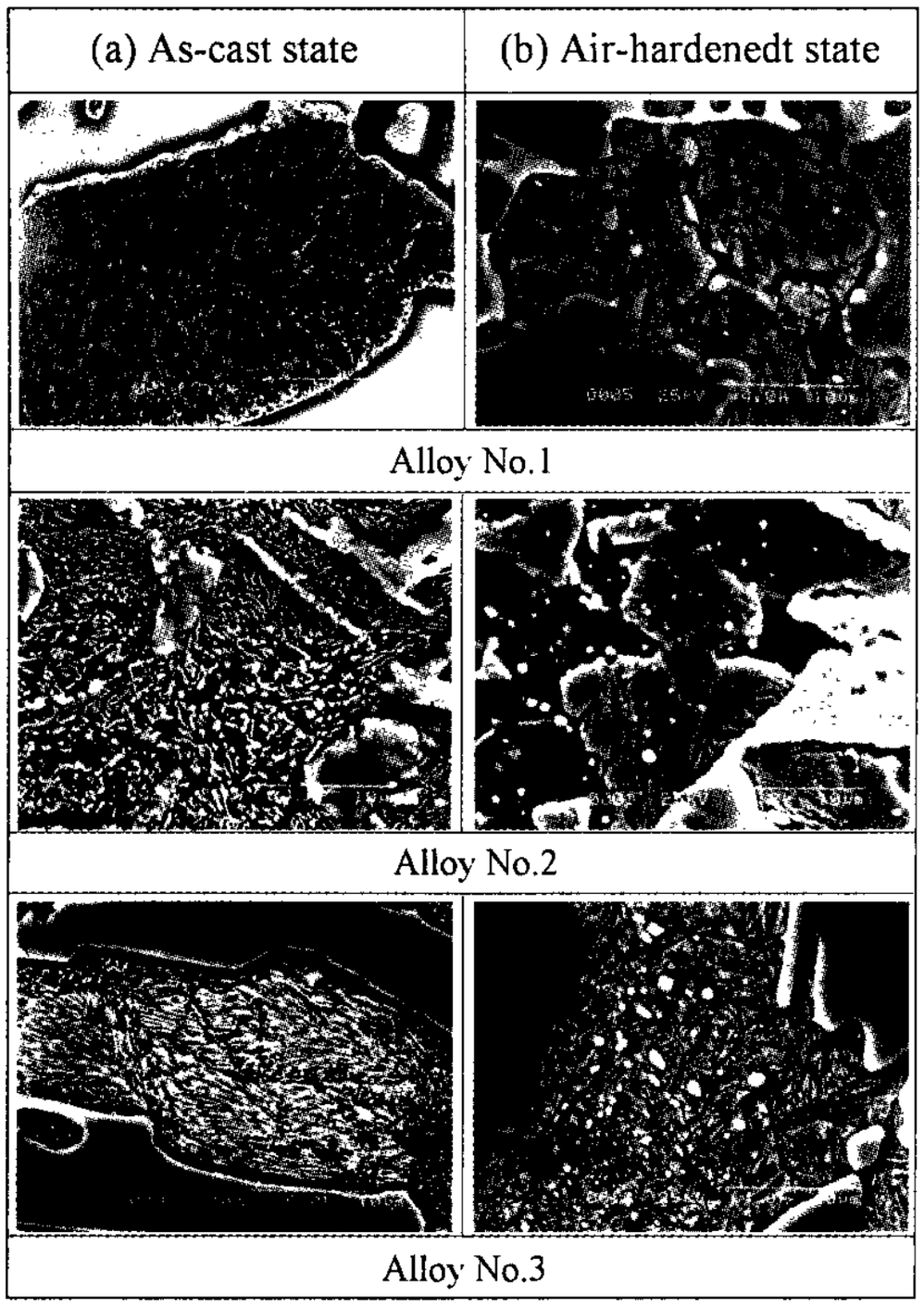

Fig. 5. Matrix microstructures in as-cast(a) and air-harde ned (b) states.

No.3 shows the highest Rw value in spite of its highest macrohardness of HV842. The reasons are possibly due to the fact that the large massive primary M_7C_3 carbides not only make the alloy brittle but also are broken away by spalling.

3.3 Abrasion Wear Behavior in Heat-treated State

The results of the abrasion wear test of the homogenized specimens are shown in Fig. 6. The Rw values ranged from 0.032 to 0.054 mg/s. It is clear that the abrasion wear of each alloy is increased by homogenizing when compared with that of the as-cast alloy. The Rw values increase from 0.034 to 0.052 mg/s in the alloy No.1, from 0.030 to 0.032mg/s in the alloy No. 2, from 0.045 to 0.054 mg/s in the alloy No.3. The increasing ratios are 52.9, 6.3 and 16.7%, respectively. The abrasion wear resistance increases in the order of alloy No.3, No.1 and No.2. Therefore, a similar postulation

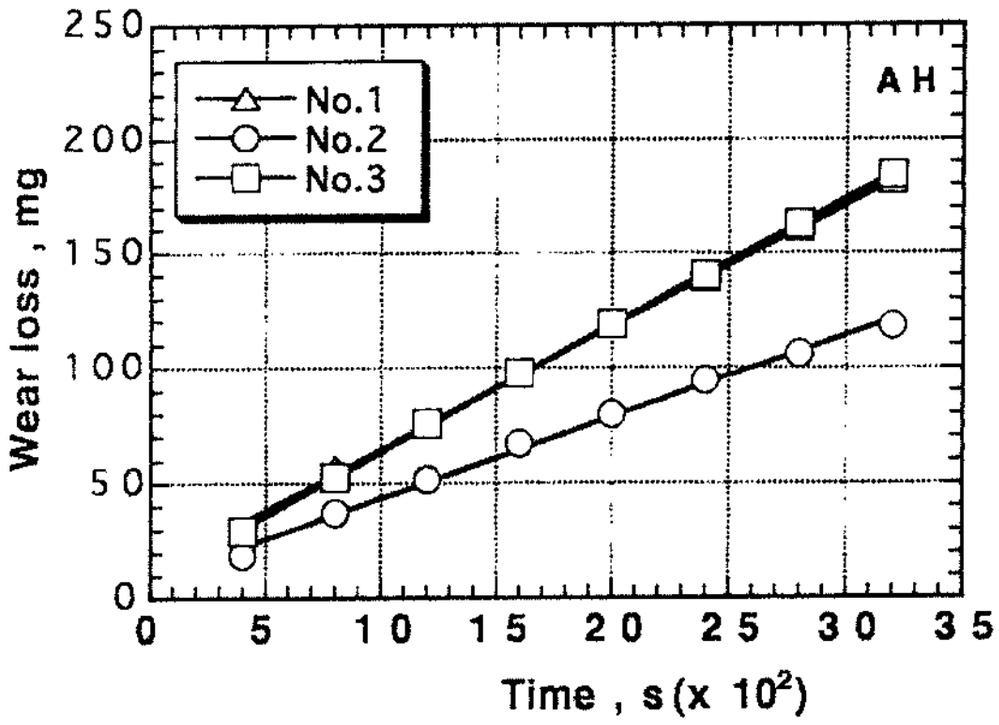

Fig. 6. Relationship between wear loss and testing time in homogenized(AH) state.

which was suggested in the as-cast state can be applied to this case. Because the matrix structures of all the homogenized specimens in this work were composed of coarse pearlite and fine secondary precipitated carbides, the macrohardness of matrix decreased greatly in comparison with that of as-cast specimens. The abrasion wear resistance of alloyed white cast iron has been generally considered to be a function of both the carbide and matrix structures, and therefore, it is natural that it decreases when the specimens are homogenized or annealed.

In case of air-hardened specimens shown in Fig. 7, the Rw values ranged from 0.009 to 0.033 mg/s indicating that the abrasion wear loss is reduced by air-hardening from 0.034 to 0.033 mg/s in the alloy No.1, from 0.030 to 0.009 mg/s in the alloy No.2, from 0.045 to 0.024 mg/

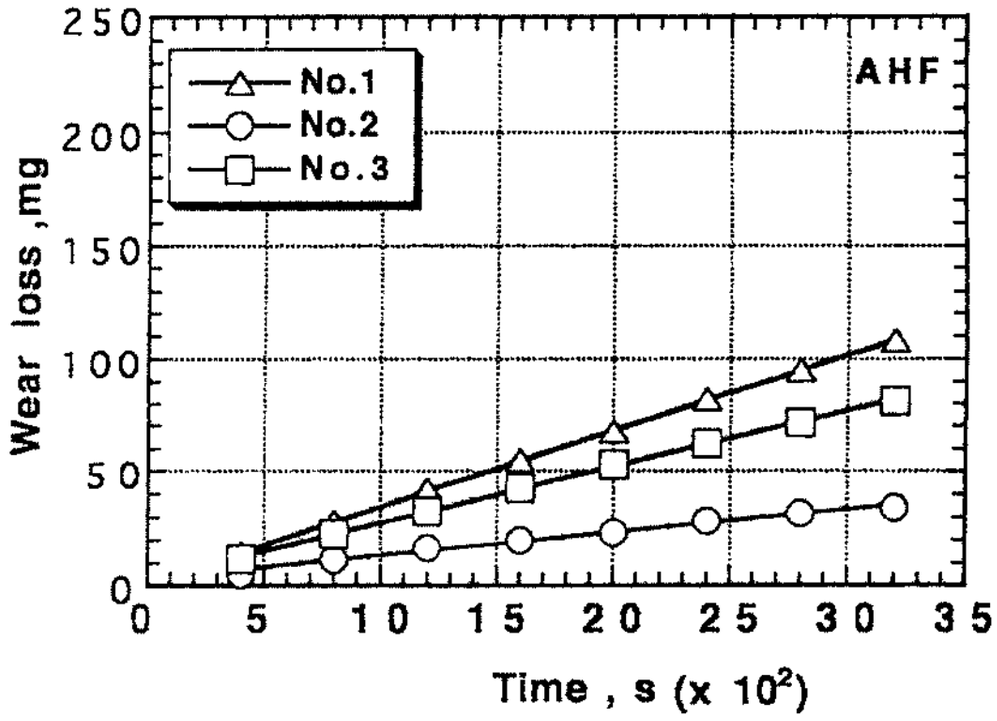

Fig. 7. Relationship between wear loss and testing time in air-hardened(AHF) state.

s in the alloy No.3, and the reduction ratios of Rw are 2.9, 70 and 46.7%, respectively. The lowest Rw value is also obtained in the alloy No.2, as was the case in the as-cast and homogenized states. However, the highest Rw value is obtained in the alloy No.1 which was ranked secondly in the as-cast and homogenized conditions. As it is distinguished qualitatively in Fig. 5(b), the Vγ value of the alloy No.1 is much higher than those of other two alloys, which corresponds to the values analyzed by X-ray diffraction. The difference in Vγ values could account for the different Rw values. It has been reported that the iron with more retained austenite shows better abrasion wear resistance under high load like 30N at the same wear test, and it can be explained by the fact that the retained austenite transforms into induced martensite by the abrasion energy or load[15]. Therefore, it is postulated that the application of 10N load might be not enough for inducing the martensite transformation from the retained austenite.

The results of abrasion wear test of the tempered specimens are also shown in Fig. 8. The Rw values ranged from 0.010 to 0.035 mg/s, indicating the abrasion wear loss is reduced remarkably in the alloy No. 2 and No.3 by tempering when compared with that of the as-cast specimen: alloy No.1(0.034→0.035 mg/s, +2.9%), alloy No.2(0.030 → 0.010 mg/s, -66.7%), alloy No.3(0.045 → 0.026mg/s, -42.2%). When it is compared with the air-hardened state, however, the abrasion wear loss of the tempered specimen increases a little in alloy No.2 and No.3 and their increasing ratios are 11.1 and 8.3%, respectively and it may be due to low tempering temperature like 573K.

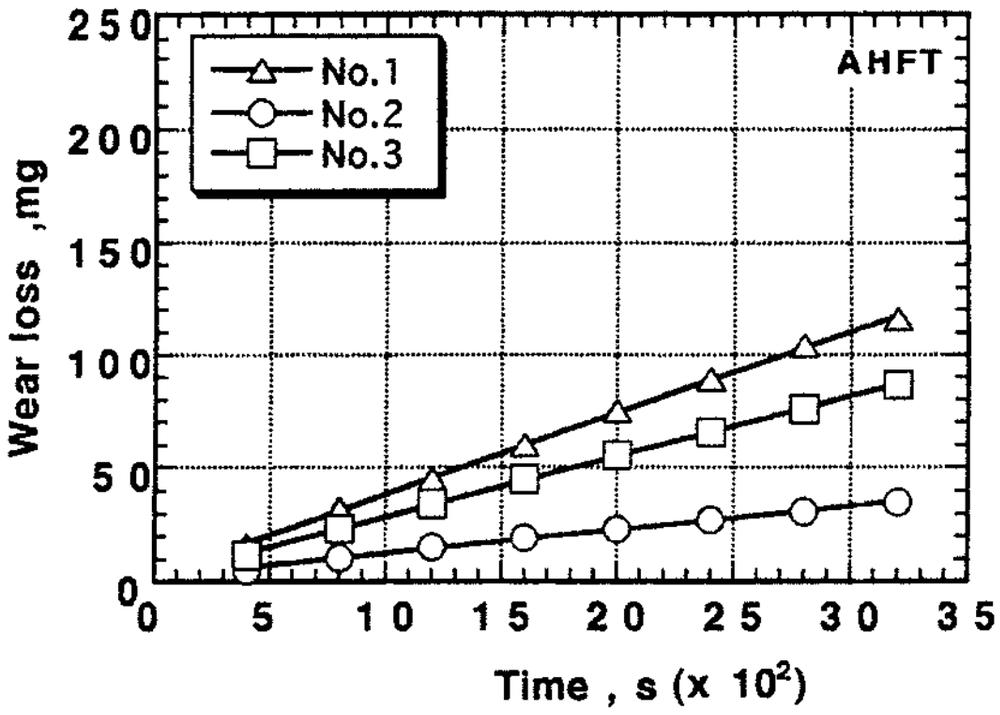

Fig. 8. Relationship between wear loss and testing time in air-hardened(AHFT) state.

3.4 Observation of Worn Surface

For more discussions about the abrasion wear behavior, the worn surface of tempered specimens were investigated using SEM. The SEM microphotographs of the worn surface and those of the cross section near the surface are shown in Fig. 9. Many scratched lines are observed on the worn surface. In the alloy No.1 which showed the worst wear resistance, many cracks caused in carbides, deep and coarse stripes in matrices can be seen. However, the worn surface of the alloy No.2 is smoother and with thin scratching lines and free of cracks. As shown clearly in the cross-sectional microstructure of this figure, the surface of matrix of the alloy No.2 is even while those of the alloys No.1 and No.3 are

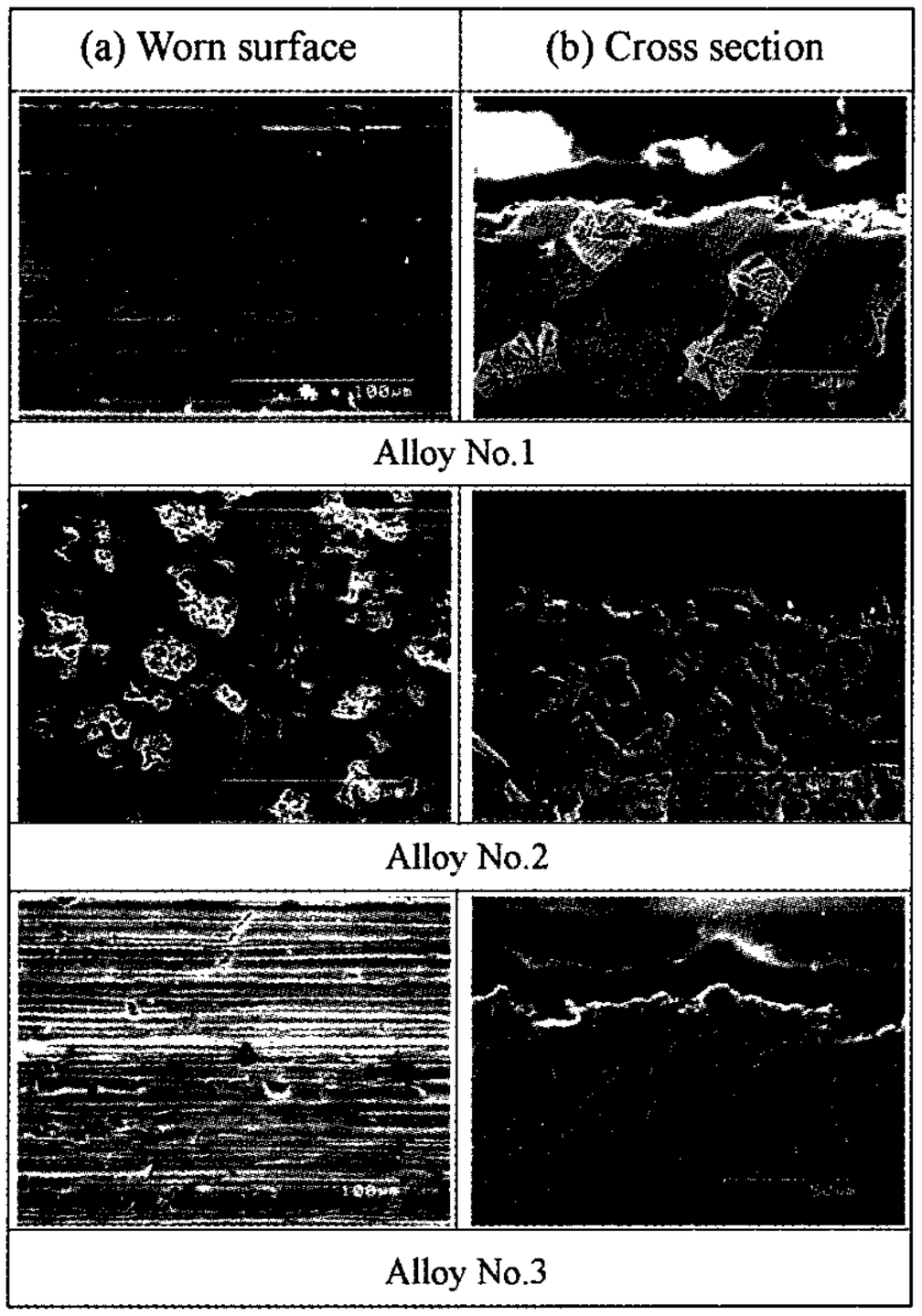

Fig. 9. SEM microphotographs of worn surface(a) and cross section to worn surhace(b) in tempered specimens.

uneven because the M_7C_3 carbides were worn away. This proves that the matrix with precipitation of hard secondary MC carbides also increases the wear resistance. As for the alloy No.1 which showed worst wear resistance, a spalling or a tearing-away can be recognized on the M_7C_3 carbides. Similar behavior is also found to occur in the alloy No.3. Therefore, it can be said from above observation that the abrasion wear of the alloys No.1 and No.3 depends mainly on massive M_7C_3 carbides while that of the alloy No.2 is mainly related to the uniform distribution of hard MC carbides.

4. Conclusions

Solidification and abrasion wear behavior of highly alloyed white cast iron has been studied. The results are summarized as follows:

1. The solidification sequence of the alloy No.1(Fe-3%C-10%Cr-5%Mo-5%W) is;

$L_0 \rightarrow$ primary $\gamma + L_1$ (R_1 at 1418K)

$L_1 \rightarrow (\gamma + M_7C_3)$ eutectic $+ L_2$ (R_2 at 1413K)

$L_2 \rightarrow (\gamma + M_6C)$ eutectic (R_3 at 1360K)

2. The solidification sequence of the alloy No.2(Fe-3%C-10%V-5%Mo-5%W) is;

$L_0 \rightarrow$ primary MC $+ L_1$ (> 1623K)

$L_1 \rightarrow$ primary $\gamma + L_2$ (R_1 at 1548K)

$L_2 \rightarrow (\gamma + MC)$ eutectic $+ L_3$ (R_2 at 1538K)

L_3 Å® (γ + M_2C) eutectic (R_3 at 1408K)

3. The alloy No. 3(Fe-3%C-17%Cr-3%V) solidified with the precipitation of primary M_7C_3 carbide followed by $(\gamma + M_7C_3)$ eutectic solidification.

4. In all the alloys, the abrasion wear loss was found to decrease in the order of homogenized(AH), as-cast (AS), tempered(AHFT) and air-hardened(AHF) states.

5. In the as-cast state, the abrasion wear loss was lowest in the alloy No.2 which was consist of primary MC carbide, eutectic MC and M_2C carbides and pearlitic matrix, and highest in the alloy No.3 having primary M_7C_3 carbide, eutectic M_7C_3 carbide and pearlitic matrix.

6. In the homogenized state, the order of the alloys in abrasion wear loss was the same as that of the as-cast state. But, the abrasion wear loss of each alloy was larger than that of each as-cast alloy because all the matrix structures were composed of coarse pearlite and fine secondary precipitated carbides.

7. In the air-hardened and tempered states, the abrasion wear loss was lowest in the alloy No.2 as was the case in the as-cast and homogenized states, and highest in the alloy No.1 having eutectic M_7C_3 and M_6C carbides and highest retained austenite in the matrix. Because of low application load like 10N, the retained austenite did not transform to martensite during abrasion wear test, which could account for the highest abrasion wear of the alloy No.1. Another reason comes from the fact that the large massive primary M_7C_3 carbides not only make the alloy brittle but also are broken away by spalling.

8. The lowest abrasion wear loss of the alloy No. 2 could be attributed to the fact that the main carbide types of this alloy are MC which has the highest hardness among the carbides in alloyed white cast iron, and M_2C with considerable amounts of W which is hardest next to the MC carbide.

Acknowledgments

This work was supported (in part) by the Korea Science and Engineering Foundation(KOSEF) through the Center for Automotive Parts Technology(CAPT) at Keimyung University.

References

[1] W. A. Fairhust, K. Rohrig: Foundry Trade Journal, 136 (1974) 685-698.

[2] J. D. Watson, P. J. Mutton: I. R. Sare, Metals Forum, 3 (1980) 74-88.

[3] K. Yamaguchi, Y. Matsubara: J. of Japan Foundrymens Society, 62 (1990) 43-49.
[4] S. K. Yu, Y. Matsubara: Proceedings of the 3rd Asian Foundry Congress, Kyungju, Korea, 1995, 128 p.
[5] Y. Matsubara, N. Sasaguri, M. Hashimoto: Proceedings of the 4th Asian Foundry Congress, Queensland, Australia, 1996, 251 p.
[6] K. Shimizu, N. Sasaguri, Y. Matsubara: Proceedings of the 4th Asian Foundry Congress, Queensland, Australia, 1996, 283 p.
[7] Y. Matsubara, N. Sasaguri: J. of Japan Foundry Engineering Society, 68 (1996) 1099-1105.
[8] Y. Honda, Y. Matsubara: Proceedings of the 5th Asian Foundry Congress, Nanjing, China, 1997, 162 p.
[9] S. K. Yu, Y. Matsubara: Proceedings of the 4th Asian Foundry Congress, Queensland, Australia, 1996, 291 p.
[10] K. H. Zum, G. H. Eldis: Wear, 64 (1980) 175-194.
[11] J. T. H. Pearce: AFS Trans., 92 (1984) 599-622.
[12] Y. Matsubara, K. Ogi, K. Matsuda: AFS Trans., 89 (1981) 183-196.
[13] H. Q. Wu, N. Sasaguri, Y. Honda, Y. Matsubara: Proceedings of the 2nd Asian Foundry Congress, Kitakyushu, Japan, 1994, 109p.
[14] H. Q. Wu, N. Sasaguri, Y. Matsubara, M. Hashimoto: AFS Trans., 104 (1996) 103-108.
[15] S. K. Yu, N. Sasaguri: Y. Matsubara, Intl. J. of Cast Metals Research, 11 (1999) 561-566.